

Stormwater infiltration and surface runoff pollution reduction performance of permeable pavement layers

Zhi-Guang Niu¹ · Zhi-Wei Lv¹ · Ying Zhang² · Zhen-Zhen Cui³

Received: 7 March 2015 / Accepted: 21 September 2015 / Published online: 2 October 2015
© Springer-Verlag Berlin Heidelberg 2015

Abstract In this paper, the laboratory-scale permeable pavement layers, including a surface permeable brick layer, coarse sand bedding layers (thicknesses=2, 3.5, and 5 cm), and single-graded gravel sub-base layers (thicknesses=15, 20, 25, and 30 cm), were built to evaluate stormwater infiltration and surface runoff pollution reduction performance. And, the infiltration rate (I) and concentrations of suspended solids (SS), total phosphorus (TP), chemical oxygen demand (COD), ammonia nitrogen, and total nitrogen (TN) were measured under the simulated rainfall intensity of 72.4 mm/h over duration of 60 min. The results indicate that the thickness factor primarily influences the infiltration rate and pollutant removal rate. The highest steady infiltration rate was for surface brick layer 51.0 mm/h, for 5-cm sand bedding layer 32.3 mm/h, and for 30-cm gravel sub-base layer 42.3 mm/h, respectively. The SS average removal rate was relative higher (79.8~98.6 %) for all layers due to the interception and filtration. The average removal rates of TP and COD were for surface layer 71.2 and 24.1 %, for 5-cm bedding layer 54.8 and 9.0 %, and for 20-cm sub-base layer 72.2 and 26.1 %. Ammonia nitrogen and TN cannot steadily be removed by layers according to the experiment results. The optimal

thickness of bedding sands was 5 cm, and that of sub-base gravels was 20~30 cm.

Keywords Permeable pavement · Infiltration rate · Pollutant removal rate · Mechanism · Rainfall duration · Structural layer parameter

Introduction

Pervious pavements have become one of the most used sustainable urban drainage system (SUDS) techniques and have strong ability in the reduction of runoff and pollutants (Brattebo and Booth 2003; Dreelin et al. 2006; Tota-Maharaj and Scholz 2010; Sanudo-Fontaneda et al. 2013, 2014a). Many studies have studied pervious pavements, mainly focusing on (1) the infiltration capacity and pollutant removal rates of the entire permeable pavement structure (Brattebo and Booth 2003; Kuang and Fu 2013; Sanudo-Fontaneda et al. 2014a, b), (2) the decrease of the infiltration capacity due to surface clogging (Fassman and Blackbourn 2010; Coughlin et al. 2012; Sanudo-Fontaneda et al. 2013; Kuang and Fu 2013), and (3) the qualitative impacts of various factors (e.g., retention time, flow rate, season, dry time, and types of materials) on the average removal rates of pollutants (Dierkes et al. 2002; Cates et al. 2009; Tota-Maharaj and Scholz 2010). However, questions that remain unanswered include (1) the study of the influence of the thickness factor on the stormwater infiltration and surface runoff pollution reduction performances in several layers of the permeable pavement systems, and (2) the variations and mechanisms of water infiltration rates and pollutant removal rates of each layer over the rainfall duration.

In this paper, the small-scale permeable pavement layers, including a surface permeable brick layer, coarse sand

Responsible editor: Philippe Garrigues

✉ Ying Zhang
zhangying@nankai.edu.cn

¹ School of Environmental Science and Engineering, Tianjin University, Tianjin 300072, China

² College of Environmental Science and Engineering, Nankai University, Tianjin 300071, China

³ China Shanghai Architectural Design & Research Institute Co., Ltd., Shanghai 200063, China

Table 1 Characteristics of each structural layer in the permeable pavement

Layer	Permeable bricks	Sand bedding	Gravel sub-base
Material	Ceramic permeable brick	Coarse sand	Single-graded gravel
Size or thickness	20 cm×20 cm×5.5 cm	2 cm, 3.5 cm, 5 cm	15 cm, 20 cm, 25 cm, 30 cm
Particle size	2~5 mm	in Table 2	5~10 mm
Porosity	NA	39.8 %	44.6 %
Water absorption	8.5 %	NA	NA
Fineness modulus	NA	2.7	NA

NA not available

bedding layers (thicknesses=2, 3.5, and 5 cm), and single-graded gravel sub-base layers (thicknesses=15, 20, 25, and 30 cm), were built to analyze the stormwater infiltration and surface runoff pollution reduction of each layer. This study sought to measure the stormwater infiltration and surface runoff pollution reduction of individual layer of permeable pavement and determine the effect of thickness on the water infiltration and pollution reduction. Moreover, the variation of the stormwater infiltration rate and pollutant removal rate of each layer over the rainfall duration was also examined.

This research could give aid to the design of the permeable pavement system for better efficiency of stormwater infiltration and pollution reduction and potentially promote the understanding of water infiltration and pollution reduction of the entire permeable pavement.

Materials and methods

Experimental materials

The permeable pavement layers were designed in accordance with the Engineering Technical Code for Rain Utilization in Building and Sub-District (GB 50400-2006) (Ministry of Construction of the People’s Republic of China 2008) (shown in Table 1). The ceramic permeable brick has a compressive strength of 48.9 MPa, a bending strength of 7.8 MPa, and a permeation coefficient of 0.0312 cm/s. They were laid flat by using a rubber hammer without damaging the corner of the bricks. Roughness deviation was not more than 5 mm, and the elevation difference between two adjacent bricks was not more than 2 mm. The coarse sand in experiment has a mud content of 0.9 %, a clod content of 0.4 %, a flat and elongated particle content of 9.5 %. The coarse sand bedding layer was also laid flat and slightly hand-compacted. The single-graded gravel used in this experiment has a mud content of 1.6 %, a clod content of 0.7 %, a flat and elongated particle content of 1.8 %. The gravel sub-base layer was compacted by grinding with thickness deviation less than 20 mm.

Experimental setup

The layer with a specific depth was laid in a plastic container with dimensions of 75.5 cm long×55 cm wide×48 cm deep. An outlet pipe with a diameter of 2 cm was installed at the bottom of the container, and a 1 % slope was applied in the horizontal direction to ensure smooth drainage. The rain was simulated with a single pipe with six nozzles that can cover the whole pavement surface. The rainfall intensity range of the screw rotating sprayer could be adjusted from 15 to 200 mm/h. The pipe was connected to a water pump with a flowmeter to control the spray speed and monitor the rainfall intensity. The flow rate range of the flowmeter (LZB-10 glass rotameter) is 6~60 L/h (shown in Fig. 1).

Test methods

According to the Engineering Technical Code for Rain Utilization in Building and Sub-District (GB 50400-2006) (Ministry of Construction of the People’s Republic of China 2008), the rainfall should be determined in terms of local rainfall data of more than 10 years, and the rainfall intensity should be more than 2 years of return period. Consequently, a rainfall of 60-min duration was simulated using the rainfall intensity of a 20-year return period in Tianjin ($q=201.14\text{ L/(s}\cdot\text{ha)}$). Several studies have found that suspended solids (SS), total phosphorus (TP), chemical oxygen demand (COD), ammonia nitrogen, and total nitrogen (TN) were the main pollutants in stormwater runoff in the urban area (Brezonik and Stadelmann 2002; Gnecco et al. 2005; Shen et al. 2009; Zhang and Li 2008). So these water quality parameters were chosen to be investigated in this paper. Raw water (influent water) was

Table 2 Particle size distribution of the sand in the bedding layer

Sieve size (mm)	9.5	4.75	2.36	1.18	0.6	0.3	0.15
Aggregate gradation (% passing sieve)	100	94	83	67	48	16	2

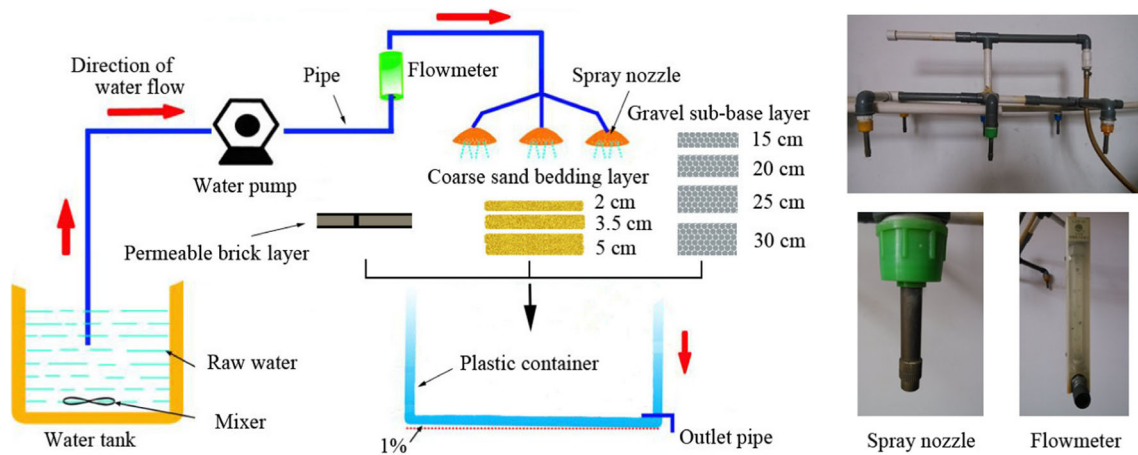


Fig. 1 Schematic diagram of the experimental setup

prepared based on the traditional surface runoff measurements from July to September 2012 in Tianjin, in North China (Table 3), and stored in a 50-L water tank before each test. The sediment used in the simulated rainfall was kaolin, which particle size distribution is shown in Fig. 2. The chemicals were all purchased from chemical network management platform of Tianjin University (<http://219.243.47.181/chem>).

The rain began spraying down from nozzles to initiate the timing, and the outflow was taken at 5-min intervals referring to the previous research studies by Bean et al. (2007), Hu (2009), Yang et al. (2013), and Zhou (2007). The effluent volume and sampling time were recorded simultaneously. Stirring was always conducted to avoid natural sedimentation of SS and nonuniform concentration of pollutants in raw water, and the laboratory conditions were controlled during the tests (temperatures 18~23 °C, humidity 70~80 %). Eight permeable pavement-layer experiments were carried out, and each one was repeated three times for improving the subsequent statistical analysis of the results in this study (shown in Table 4). In addition, The event mean concentration (EMC) of effluent volume and various pollutants from each layer was

Table 3 Raw water quality

Items	Traditional runoff (mg/L)	Raw water (mg/L)	Reagent
SS	31~1020	648	Kaolin
COD	18~276	244	Glucose
TP	0.25~1.44	1	Na ₂ HPO ₄
Ammonia	1.68~18	7	NH ₄ Cl
TN	3.32~27.13	11	NaNO ₃ , NH ₄ Cl

SS suspended solids, TP total phosphorus, COD chemical oxygen demand, TN total nitrogen

calculated to analyze the infiltration rate and pollutant removal rate. The water quality was analyzed within 24 h after sampling, and the measurement methods are shown in Table 5.

Statistical analysis

The results of effluent volume and pollutant concentration were processed by EXCEL2010, and figures between infiltration rate and both pollutant removal rate and rainfall duration were generated by ORIGIN8.0 software.

Quality assurance

All the samples and blanks were analyzed in duplicates for quality assurance control of laboratory analyses in this study. Only the relative standard deviation (RSD) values below 10 % were accepted, while other samples outside this range were

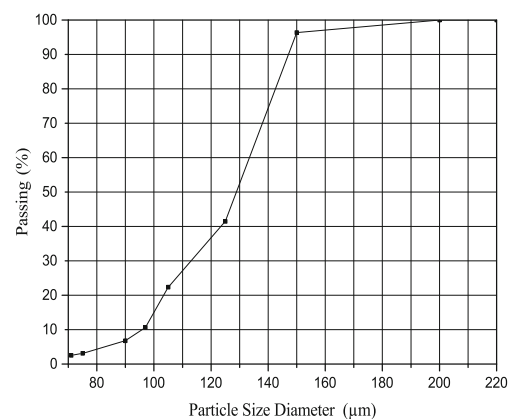


Fig. 2 Particle size diameter distribution of the kaolin in the simulated rainfall

Table 4 The number of tests and repetitions carried out for each layer during the research

Test number	Layer	Repetition number
1	Permeable bricks	3
2	2 cm bedding sands	3
3	3.5 cm bedding sands	3
4	5 cm bedding sands	3
5	15 cm sub-base gravels	3
6	20 cm sub-base gravels	3
7	25 cm sub-base gravels	3
8	30 cm sub-base gravels	3

reanalyzed. A standard reference material (SRM) GSB 07-1982-2005 from Institution for Environmental Reference Material Ministry of Environmental Protection was applied for calibration and analytical control. The parameters were identified relative to external standards. The detection limits of TP, COD, ammonia nitrogen, and TN were 0.01, 15, 0.025, and 0.05 mg/L, respectively.

Results and discussion

Permeable brick layer

Infiltration rate of the permeable brick layer

The infiltration rate of the permeable bricks is shown in Fig. 3. The steady infiltration rate of the brick pavers was 51.0 mm/h, and no outflow was observed before 5 min. The outflow will occur when the permeable bricks are dripping wet. About 10 min later, the infiltration rate became steady and approached the saturated hydraulic conductivity, which confirmed the results from Davies et al.

Table 5 Laboratory methods used in analysis of samples

Items	Method
SS	Gravimetric method (GB 11901-89)
COD	Fast digestion-spectrophotometric method (HJ/T 399-2007)
TP	Ammonium molybdate spectrophotometric method (GB 11893-89)
Ammonia	Nessler’s reagent spectrophotometry (HJ 535-2009)
TN	Alkaline potassium persulfate digestion UV spectrophotometric method (HJ 636-2012)

SS suspended solids, TP total phosphorus, COD chemical oxygen demand, TN total nitrogen

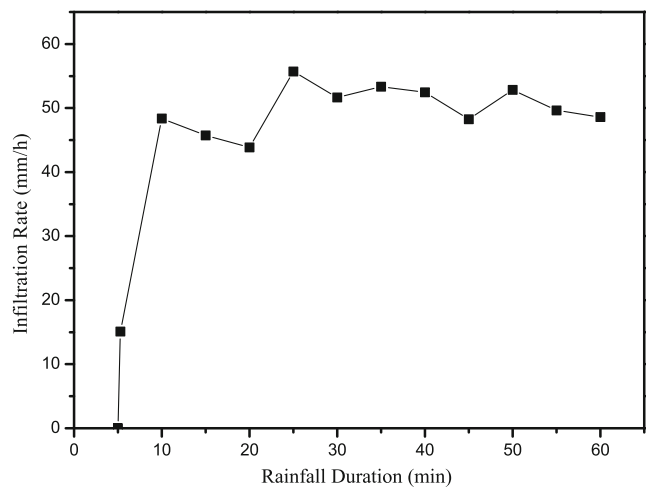


Fig. 3 Infiltration rate of the permeable bricks

(2002), Nnadi et al. (2014), Rodriguez-Hernandez et al. (2012), and Sanudo-Fontaneda et al. (2013) regarding with the time needed to reach the steady state.

Pollutant removal of the permeable brick layer

The pollutant removal rates of the permeable brick layer as a function of the rainfall duration are shown in Fig. 4, and the water quality of the effluent is shown in Figs. 5, 6, 7, 8, and 9.

The average removal rate of SS was 79.8 %. The bricks rapidly removed particles by filtration, sorption, and interception (Hou 2008).

The average removal rate of TP was 71.2 %. The calcium components in the ceramic permeable bricks could adsorb part

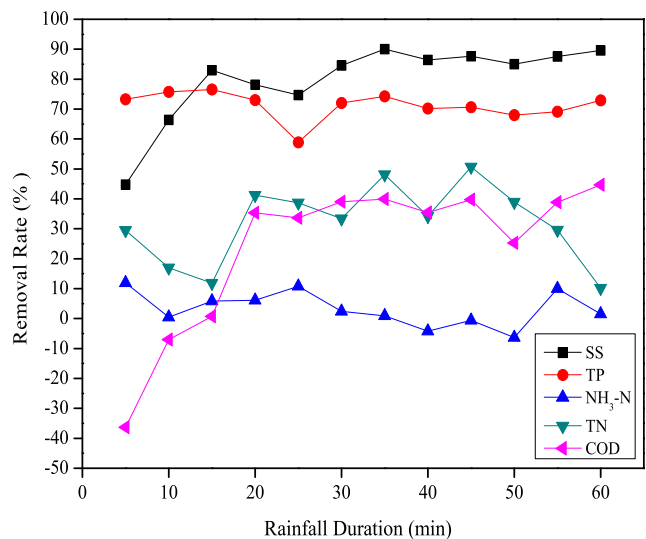
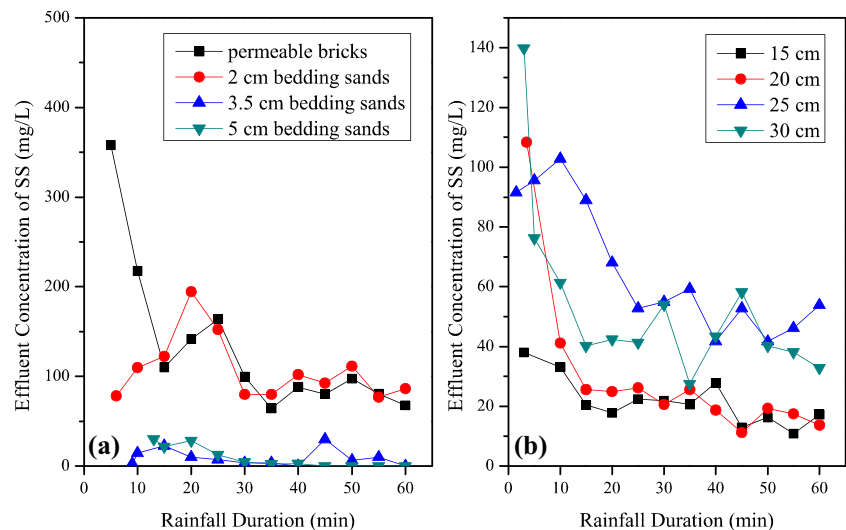


Fig. 4 Pollutant removal rates of the permeable bricks

Fig 5 Effluent concentration of SS over the rainfall duration from **a** permeable bricks and bedding sands and **b** sub-base gravels



of the phosphorus (Geller 1997; Zhu 1999). The change in the TP removal rate was consistent with that of the SS, which indicates that TP could also be adsorbed by particles, consistent with the conclusions of Xiong (2007), Cates et al. (2009), and Eck et al. (2012).

The average removal rate of COD was 24.1 %. The removal rate was negative during the first 15 min because residual organics previously deposited in the permeable bricks desorbed by scouring. Then, the removal rate increased and ultimately stabilized due to reaching an adsorption-desorption balance (Hou 2008).

The average removal rate of ammonia nitrogen was 3.25 %. Kaolin performed the function of cation exchange (Han 2007), so ammonia was removed mainly through ion exchange. However, only a small amount of ammonia was

removed because of the limited number of ion sites (Han 2007). The average removal rate of TN was 3.25 %, consisted with Eck et al. (2012).

Sand bedding layer

Infiltration rate of the sand bedding layer

The infiltration rates of sand bedding layers with three different thicknesses are shown in Fig. 10. The steady infiltration rates of different thicknesses in descending order are 32.3 mm/h (5-cm layer) > 30.9 mm/h (2-cm layer) > 24.5 mm/h (3.5-cm layer). In the 2-cm layer, the water infiltration rate was more prominently influenced by gravity during the initial 20 min because fewer particles were intercepted than for the other

Fig 6 Effluent concentration of TP over the rainfall duration from **a** permeable bricks and bedding sands and **b** sub-base gravels

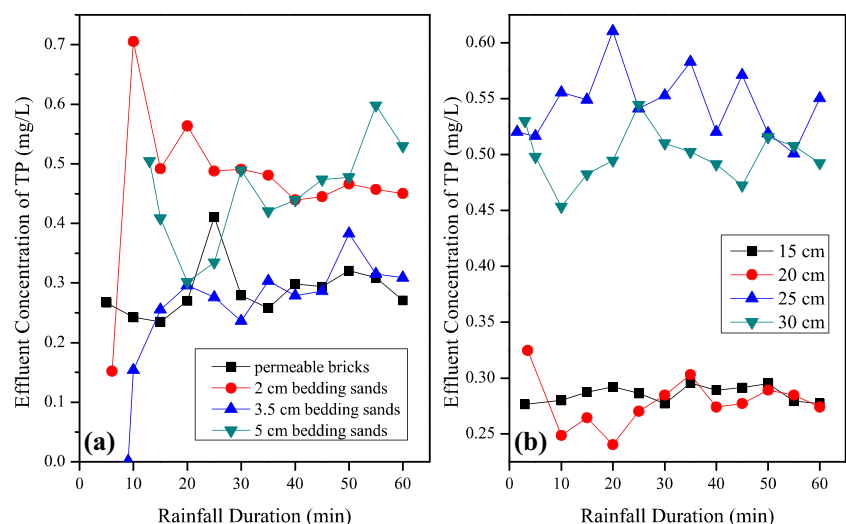
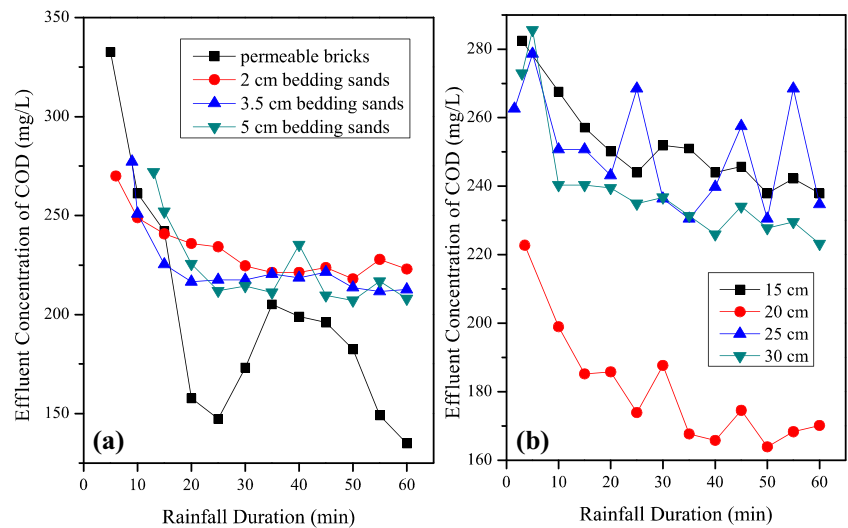


Fig 7 Effluent concentration of COD over the rainfall duration from **a** permeable bricks and bedding sands and **b** sub-base gravels



thicknesses (Figs. 5a and 11) (Pan et al. 2010). Gravitational drainage can drive the lower water to move quickly under the hydrodynamic pressure (Zhang 2005; Liu 2008), and in consequence, the infiltration rate increased dramatically. The infiltration rate decreased soon afterward because the air in the structure could not exhaust effectively under the rapid flow of water (Lv and Hao 2008). After that, the matric suction increased and the gravity weakened due to the increase of the particulate matter filtered (Liu 2008; Pan et al. 2010). The infiltration rate of the 5-cm layer was similar to that of the 2-cm layer. It could be concluded that no air was retained in the 3.5- and 5-cm layers because during the initial 30 min, more particles were retained in the two layers than in the 2-cm layer (Figs. 5a and 11), so no rapid flow appeared. The matric suction was more obvious in the 3.5-cm layer because of the

particles accumulated; moreover, the effect of the suction is weaker than that of gravity (Pan et al. 2010), so the infiltration rate of the 3.5-cm layer increased slowly.

Pollutant removal of sand bedding layer

The pollutant removal rates of the sand bedding layers are shown in Table 6, and the water quality of the effluent are shown in Figs. 5, 6, 7, 8, and 9. The removal rates of SS, COD, and ammonia nitrogen of the 5-cm layer were higher than those of the 3.5- and 2-cm layers, while the removal rate of TP in the 3.5-cm layer was the highest. The sand bedding layer could hardly remove TN.

The removal rates of SS and TP in the sand bedding layers of three thicknesses are shown in Fig. 11. The infiltration rate

Fig 8 Effluent concentration of ammonia over the rainfall duration from **a** permeable bricks and bedding sands and **b** sub-base gravels

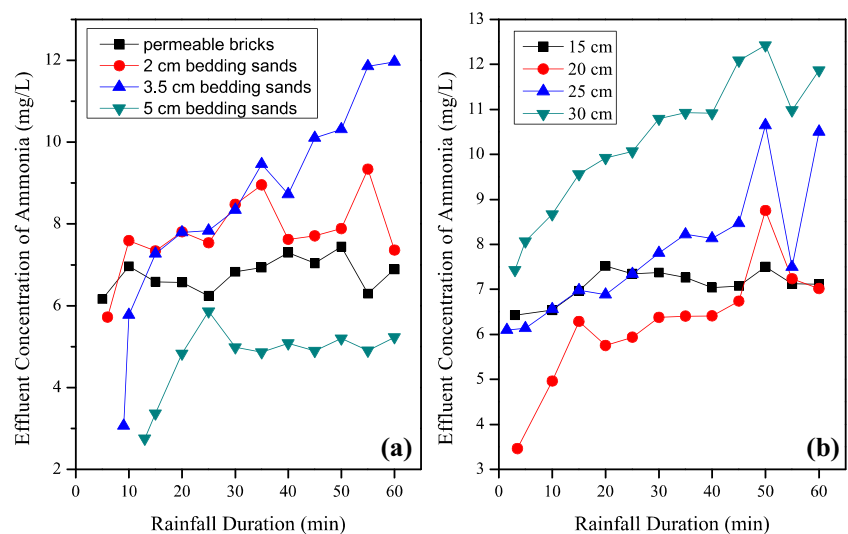
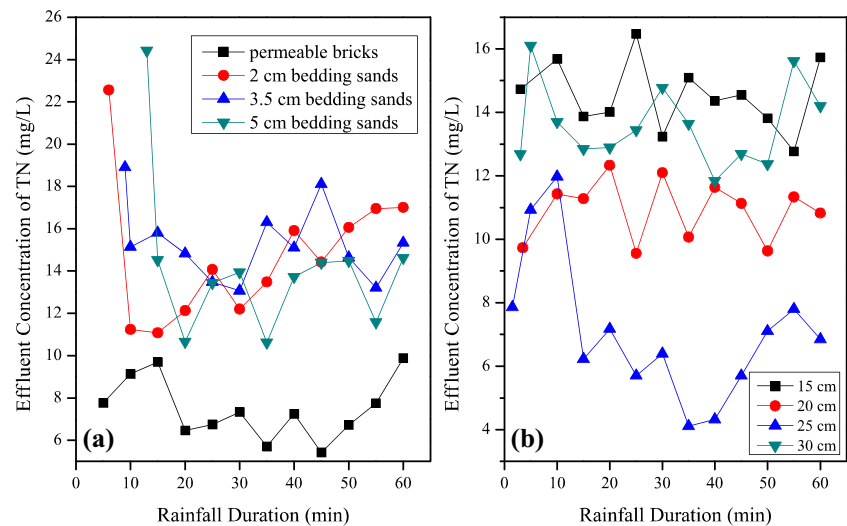


Fig 9 Effluent concentration of TN over the rainfall duration from **a** permeable bricks and bedding sands and **b** sub-base gravels



of the 2-cm layer was much higher than that of the 3.5- and the 5-cm layers during the first 20 min (Fig. 10). The rapid movement of water affected the adsorption and retention of SS, leading to a sharp decline in its removal. In addition, the removal of TP was mainly dependent on adsorption of particles (Xiong 2007; Cates et al. 2009; Tota-Maharaj and Scholz 2010; Eck et al. 2012). So there was a significant amount of TP captured as SS washed out at this period (Figs. 6a and 11), leading to the dramatic increase of its effluent concentration (Fig. 6a). Then, with the decrease of the infiltration rate, the removal rate of SS increased and reached a steady state after 30 min. The similar situation happened on the removal rate of TP from 2-cm bedding sands meanwhile. The removal rate of TP in the 3.5-cm layer was the highest because of the significant quantity of retained particles and the lowest infiltration

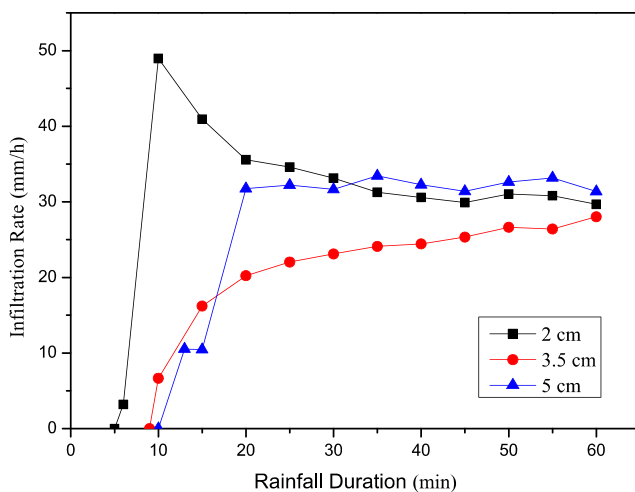


Fig. 10 Infiltration rates of the sand bedding layers with different thicknesses

rate (Xiong 2007; Cates et al. 2009; Tota-Maharaj and Scholz 2010; Eck et al. 2012).

The COD removal rates in the sand bedding layers are shown in Fig. 12a. COD was removed rapidly because of the adsorbent site vacancies in sand during the early stage of precipitation. Soon after, the removal rates increased slowly with the decrease of the adsorption sites and ultimately reached a steady state. Srimurali et al. (1998) studied the removal of fluorides by adsorption onto bentonite and charfines and reached similar conclusions.

The effluent pH varied from 5 to 7.85, and ammonia exists mainly in ionic form under these conditions (Li et al. 2007), so the ammonia could be removed by cation exchange with kaolin (Han 2007). However, the ion exchange capacity of kaolin is limited (Han 2007), so the removal rate of ammonia declined significantly as the rainfall continued. The removal rate of ammonia in the 5-cm layer was slightly higher than that in the other thicknesses due to the great amount of adsorbent. It could be concluded from Fig. 13 that nitrate was prone to be desorbed by flushing and could not be removed in the sand bedding layers. Figure 13 indicates that the effluent of TN was influenced mostly by nitrate during the initial 20 min and thereafter by both nitrate and ammonia.

Gravel sub-base layer

Infiltration rate of the gravel sub-base layer

The infiltration rates of gravel sub-base layers of four thicknesses are shown in Fig. 14. The steady infiltration rate of each layer in descending order was 42.3 mm/h (30 cm) > 36.7 mm/h (25 cm) > 27.3 mm/h (15 cm) >

Fig. 11 The removal rates of SS and TP in sand bedding layers of three thicknesses

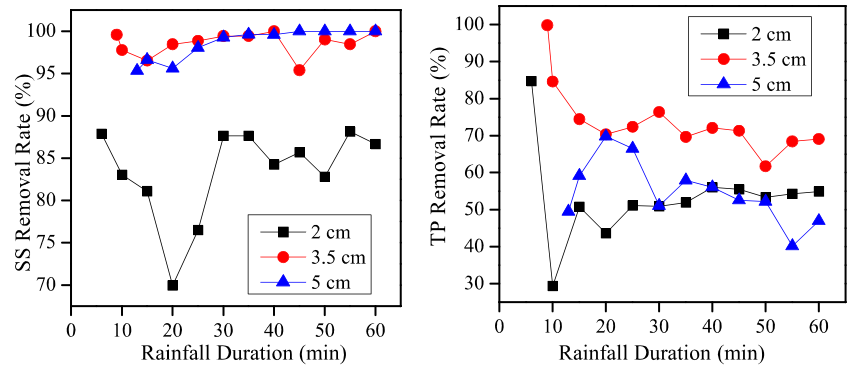


Table 6 Pollutant removal rates of sand bedding layers with three thicknesses

Items	Removal rate range (%)			Mean (%)		
	2 cm	3.5 cm	5 cm	2 cm	3.5 cm	5 cm
SS	70.0~88.1	95.4~100	95.4~100	83.5	98.6	98.6
COD	-10.6~10.6	-13.7~13.3	-11.5~15.1	4.7	7.7	9.0
TP	29.5~84.8	61.7~99.9	40.2~69.8	53.1	74.2	54.8
Ammonia	-27.9~18.3	-11.9~56.2	16.3~60.6	-10.3	1.04	32.5
TN	-105.1~-0.7	-71.9~-18.8	-122.0~3.5	-34.2	-39.3	-29.3

SS suspended solids, TP total phosphorus, COD chemical oxygen demand, TN total nitrogen

19.5 mm/h (20 cm). The infiltration rates of the 25- and 30-cm layers were higher than those of the 15- and 20-cm layers during the first 30 min because the former two depths were less clogged (Figs. 6b and 15). Thereafter, the infiltration rates increased slowly with the accumulation of particles. The infiltration process of the 15- and 20-cm gravel sub-base layers was consistent with that of the 3.5-cm sand bedding layer because of particle accumulation.

Pollutant removal of the gravel sub-base layer

The pollutant removal rates of gravel sub-base layers of four thicknesses are shown in Table 7, and the water quality of the effluent are shown in Figs. 5, 6, 7, 8, and 9. For the removal of TP, COD, and ammonia, the 20-cm layer was higher than the others, while the 15-cm layer was highest for SS removal. For TN, there was no stable removal observed.

Fig. 12 COD removal rates in a sand bedding layers and b gravel sub-base layers

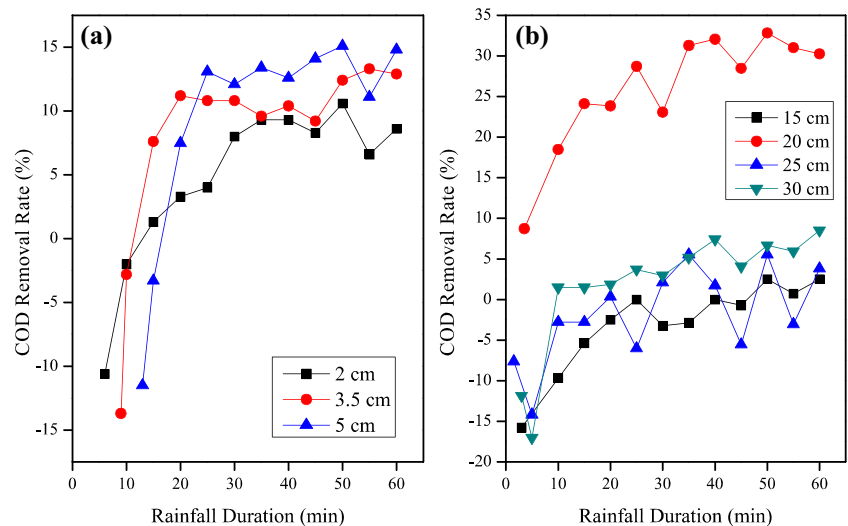
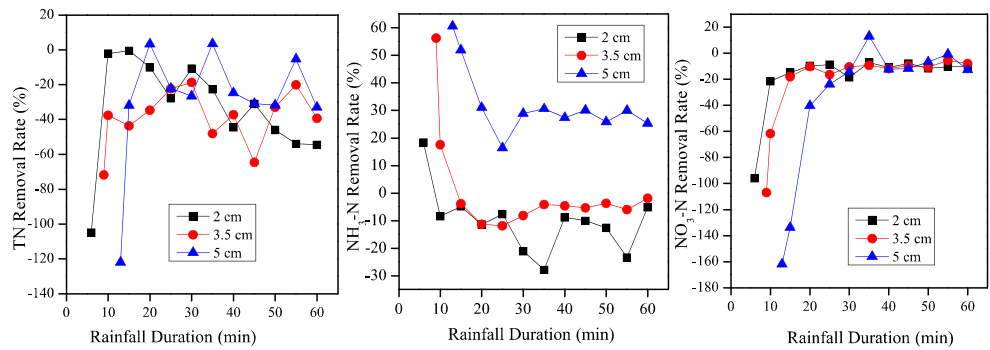


Fig. 13 Removal rates of ammonia, TN, and NO₃-N in sand bedding layers of three thicknesses



High flow rates would reduce the adsorption and sedimentation of media to particles, so the SS removal rates of the 15- and 20-cm layers were higher than those of the others. The TP removal rates of the 15- and 20-cm layers were significantly higher than those of the other two layers, which was consistent with the SS removal rates. Hence, it could be concluded that TP was also adsorbed by particles in the gravel sub-base layer (Fig. 15).

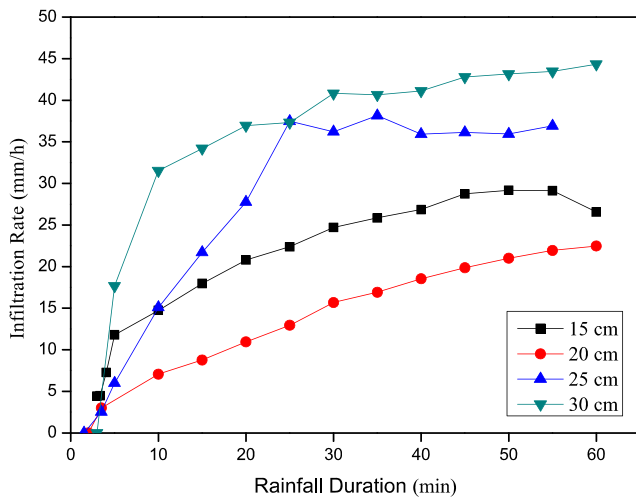


Fig. 14 Infiltration rates of gravel base layers of different thicknesses

The removal rates of COD in the gravel sub-base layers are shown in Fig. 12b. The removal rate of COD in the 20-cm layer was higher than that of the others because the worst infiltration in the 20-cm sub-base layer favored the adsorption and interception of COD (Hou 2008; Fig. 14).

The infiltration rates were higher in the 25- and 30-cm layers (Fig. 14), which weakened the adsorption and ion exchange (Hou 2008), so the removal rates of ammonia dropped more quickly in the 25- and 30-cm layers than those in the 15- and 20-cm layers (Fig. 16). The results show that the removal rate of TN was the highest in the 25-cm layer, and no removal was observed in the other layers (Fig. 16).

Comprehensive analysis

There was no surface runoff produced in the permeable bricks and sub-base gravels during the experiment. Thus, the reduction of runoff is more effective in the surface and sub-base layers than in the entire pavement structures reported by Rushton (2001) (50 %), Gilbert and Clausen (2006) (72 %), Dreelin et al. (2006) (93 %), and Collins et al. (2008) (98 %). This is because the single layer has a shorter distance and higher porosity than the entire permeable pavement. However,

Fig. 15 SS and TP removal rates in gravel base layers of four thicknesses

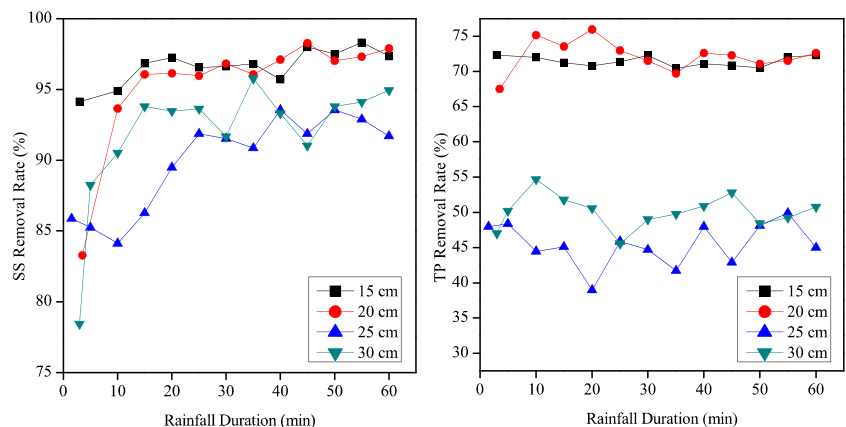


Table 7 Pollutant removal rates in base gravel layers with four different thicknesses

Items	Average removal rate (%)				Removal rate range (%)			
	15 cm	20 cm	25 cm	30 cm	15 cm	20 cm	25 cm	30 cm
SS	96.9	95.5	89.9	91.7	94.1~100	83.2~98.3	84.1~93.6	78.4~95.8
COD	-2.9	26.1	-1.76	1.57	-15.8~2.5	8.7~32.8	-14.2~5.5	-17.0~8.5
TP	71.4	72.2	45.5	50.0	70.4~72.3	67.5~76.0	39.0~50.0	45.6~54.7
Ammonia	-1.55	10.30	-11.3	-46.9	-7.45~8.19	-25.0~50	-52.1~12	-77.5~-6.1
TN	-32.1	0.71	35.6	-23.7	-49.8~-16.1	-12.1~13	-8.9~62.6	-46.4~-7.7

a small amount of runoff existed in the sand bedding layer during the test. This suggests that the bedding layer was a main limiting factor for water infiltrating into the entire permeable pavement, and the sub-base layer played a major role in determining the water storage capacity of the permeable pavement, which is consistent with the study by Park et al. (2014).

The removal rates of SS from the permeable pavement layers agreed with the observations on permeable pavement by Pezzaniti et al. (2009) (94 %), Tota-Maharaj and Scholz (2010) (91 %), and Kuang and Fu (2013) (87.6 %). The removal rates of TP and ammonia were lower than those (78 % and 85 %) in the study of Tota-Maharaj and Scholz (2010). In the study of Tota-Maharaj and Scholz (2010), the depth of each layer of permeable pavement was significantly greater than that in this paper, which leads to higher capacities of adsorption, interception, filtration, and ion exchange; what is more, processes of microbial degradation and nutrient transformation such as nitrification and denitrification could also be observed during a longer rainfall period.

Conclusions

The results presented in this paper indicate that

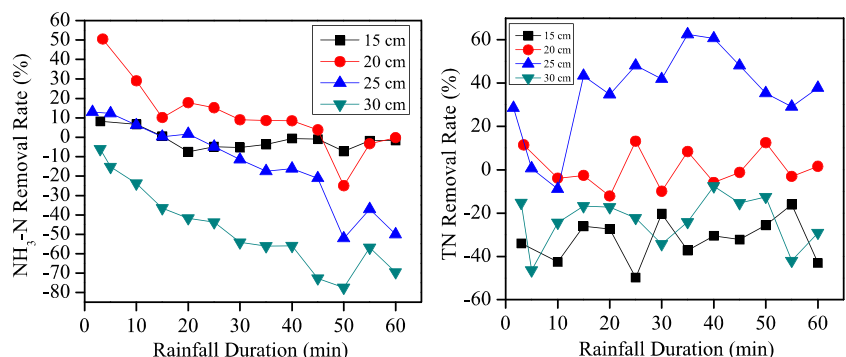
1. The steady infiltration rate of the brick pavers was 51.0 mm/h, while those of the bedding and sub-base layer

mainly depended on the thickness in this experiment. The optimal thickness of the sand bedding layer was 5 cm (the infiltration rate=32.3 mm/h), and that of the sub-base layer was 30 cm (42.3 mm/h).

2. SS could be effectively removed by all layers, with removal rates from 79.8 to 98.6 %. The 5-cm sand bedding layer had the highest removal rates for COD and ammonia nitrogen (9.0 and 32.5 %), while the 3.5-cm bedding sands had the highest removal rate of TP (74.2 %) resulted from both the retained particles and infiltration rate. The sand bedding layer could hardly remove TN. For the removal of TP, COD, and ammonia, the 20-cm gravel sub-base layer was higher than the others, with the removal rates of 72.2, 26.1, and 10.3 %. For TN, 25 cm was the optimal thickness while the removal rate reached 35.6 %.
3. Considering both the water infiltration and pollution reduction, the recommend optimal thickness of bedding sands is 5 cm, and that of sub-base gravels is 20~30 cm.

In the future, field tests will be developed to validate the results obtained in the laboratory. Also, further tests will be conducted on other surfaces and different materials for the bedding and sub-base, applying the same laboratory and statistical methodology, with the aim of characterizing the infiltration behavior of the most used permeable pavement layers across the world.

Fig. 16 Removal rates of ammonia and TN in base gravel layers of four thicknesses



Acknowledgments This research was supported by the National Natural Science Foundation of China (51308305), the National Water Pollution Control and Management Technology Major Projects of China (2014ZX07203-009), and the Program for New Century Excellent Talents in University of China. It is also very thankful for the Tianjin Urban Construction Design Institute for their help during the experiment.

References

- Bean EZ, Hunt WF, Bidelsbach DA (2007) Evaluation of four permeable pavement sites in eastern North Carolina for runoff reduction and water quality impacts. *J Irrig Drain E-Asce* 133:583–592
- Brattebo BO, Booth DB (2003) Long-term stormwater quantity and quality performance of permeable pavement systems. *Water Res* 37: 4369–4376
- Brezonik PL, Stadelmann TH (2002) Analysis and predictive models of stormwater runoff volumes, loads, and pollutant concentrations from watersheds in the Twin Cities metropolitan area, Minnesota, USA. *Water Res* 36(7):1743–1757
- Cates EL, Westphal MJ, Cox JH, Calabria J, Patch SC (2009) Field evaluation of a proprietary storm-water treatment system: removal efficiency and relationships to peak flow, season, and dry time. *J Environ Eng-Asce* 135:511–517
- Collins KA, Hunt WF, Hathaway JM (2008) Hydrologic comparison of four types of permeable pavement and standard asphalt in eastern north carolina. *J Hydrol Eng* 13:1146–1157
- Coughlin JP, Campbell CD, Mays DC (2012) Infiltration and clogging by sand and clay in a pervious concrete pavement system. *J Hydrol Eng* 17:68–73
- Davies JW, Pratt CJ, Scott MA (2002) Laboratory study of permeable pavement systems to support hydraulic modelling. Proc. of the 9th International Conf. on Urban Drainage (9ICUD), ASCE, Reston
- Dierkes C, Kuhlmann L, Kandasamy J, Angelis G (2002) Pollution retention capability and maintenance of permeable pavements. In: proceedings of Ninth International Conference on Urban Drainage, American Society of Civil Engineers, 1-13
- Dreelin EA, Fowler L, Carroll CR (2006) A test of porous pavement effectiveness on clay soils during natural storm events. *Water Res* 40:799–805
- Eck BJ, Winston RJ, Hunt WF, Barrett ME (2012) Water quality of drainage from permeable friction course. *J Environ Eng-Aace* 138: 174–181
- Fassman EA, Blackburn S (2010) Urban runoff mitigation by a permeable pavement system over impermeable soils. *J Hydrol Eng* 15: 475–485
- Geller G (1997) Horizontal subsurface flow systems in the German speaking countries: summary of long-term scientific and practical experience: recommendations. *Water Sci Technol* 35:157–166
- Gilbert JK, Clausen JC (2006) Stormwater runoff quality and quantity from asphalt, paver, and crushed stone driveways in Connecticut. *Water Res* 40:826–832
- Gnecco I, Berretta C, Lanza LG, La Barbera P (2005) Storm water pollution in the urban environment of Genoa, Italy. *Atmos Res* 77(1-4): 60–73
- Han J (2007) Process of ammonium ion-sieve's molding and its application on removal of ammonia in reclaimed water. Dissertation, Tianjin University (in Chinese)
- Hou CL (2008) Study on the treatment of polluted river water by constructed rapid infiltration system. Dissertation, Xi'an University of Architecture & Technology (in Chinese)
- Hu K (2009) Research on the water quality evaluation and use of rain on city area. Dissertation, Harbin Institute of Technology (in Chinese)
- Kuang X, Fu Y (2013) Coupled infiltration and filtration behaviours of concrete porous pavement for stormwater management. *Hydrol Process* 27:532–540
- Li Z, Fu K, Xia QB (2007) Modification of natural zeolite and adsorption of ammonia nitrogen by modified natural zeolite. *J South Chin Univ Technol (Nat Sci Edit)* 35:6–10 (in Chinese)
- Liu XP (2008) Study on the water-effects of unsaturated-soil roadbed and water-transfer characteristics in the roadbed. Dissertation, Hunan University (in Chinese)
- Lv G, Hao XY (2008) Review on influential factors of soil infiltration characteristics. *Chin Agric Sci Bull* 24:494–499 (in Chinese)
- Ministry of Construction of the People's Republic of China (2008) Engineering Technical Code for Rain Utilization in Building and Sub-District (GB 50400-2006). China Architecture & Building Press, Beijing (in Chinese)
- Nnadi EO, Coupe SJ, Sanudo-Fontaneda LA, Rodriguez-Hernandez J (2014) An evaluation of enhanced geotextile layer in permeable pavement to improve stormwater infiltration and attenuation. *Int J Pavement Eng* 15:925–932
- Pan AJ, Zhang SH, Chen JG, Ding YY (2010) Study and application on the comprehensive utilization technology of urban rainwater. China Water & Power Press, Beijing (in Chinese)
- Park DG, Sandoval N, Lin W, Kim H, Cho YH (2014) A case study: evaluation of water storage capacity in permeable block pavement. *Ksce J Civ Eng* 18:514–520
- Pezzaniti D, Beecham S, Kandasamy J (2009) Influence of clogging on the effective life of permeable pavements. *P I Civil Eng-Wat M* 162: 211–220
- Rodriguez-Hernandez J, Castro-Fresno D, Fernandez-Barrera AH, Vega-Zamanillo A (2012) Characterization of infiltration capacity of permeable pavements with porous asphalt surface using cantabrian fixed infiltrometer. *J Hydrol Eng* 17:597–603
- Rushton BT (2001) Low-impact parking lot design reduces runoff and pollutant loads. *J Water Res Pl-Asce* 127:172–179
- Sanudo-Fontaneda LA, Rodriguez-Hernandez J, Vega-Zamanillo A, Castro-Fresno D (2013) Laboratory analysis of the infiltration capacity of interlocking concrete block pavements in car parks. *Water Sci Technol* 67:675–681
- Sanudo-Fontaneda LA, Charlesworth SM, Castro-Fresno D, Andres-Valeri VCA, Rodriguez-Hernandez J (2014a) Water quality and quantity assessment of pervious pavements performance in experimental car park areas. *Water Sci Technol* 69:1526–1533
- Sanudo-Fontaneda LA, Rodriguez-Hernandez J, Calzada-Perez MA, Castro-Fresno D (2014b) Infiltration Behaviour of Polymer-Modified Porous Concrete and Porous Asphalt Surfaces used in SuDS Techniques. *Clean-Soil Air Water* 42:139–145
- Shen LQ, Che W, Li HY, He WH, Li SQ (2009) Urban road rainwater runoff pollution and its control measures in China. *China Water Wastewater* 25(4):23–28 (in Chinese)
- Srimurali M, Pragathi A, Karthikeyan J (1998) A study on removal of fluorides from drinking water by adsorption onto low-cost materials. *Environ Pollut* 99:285–289
- Tota-Maharaj K, Scholz M (2010) Efficiency of permeable pavement systems for the removal of urban runoff pollutants under varying environmental conditions. *Environ Prog Sustain* 29:358–369
- Xiong GX (2007) Research on the behavior and removal mechanism of phosphorus in wetland. Dissertation, Guangdong University of Technology (in Chinese)
- Yang X, You XY, Ji M, Nima C (2013) Influence factors and prediction of stormwater runoff of urban green space in Tianjin, China: laboratory

- experiment and quantitative theory model. *Water Sci Technol* 67: 869–876
- Zhang QG (2005) Study on the analysis methods of rainfall infiltration capacity. Dissertation, Shandong University (in Chinese)
- Zhang SN, Li XJ (2008) Pollution feature of road surface runoff in urban district of Tianjin. *Environ Sci Manag* 33(2):25–28 (in Chinese)
- Zhou YH (2007) The Simulation and control on stormwater runoff pollution of urban residential district. Dissertation, Hu Nan University (in Chinese)
- Zhu T (1999) Phosphate sorption and chemical characteristics of lightweight aggregates (LWA)-potential filter media in treatment wetlands. *Water Sci Technol* 35:103–108